THE ROLE OF VIRTUAL MASS, LIFT AND WALL LUBRICATION FORCES IN ACCELERATED BUBBLY FLOWS

Clovis R. Maliska and Emilio E. Paladino***

**Federal University of Santa Catarina*
Mechanical Engineering Department
Computational Fluid Dynamics Laboratory-SINMEC
maliska@sinmec.ufsc.br)

*** ESSS-Eng. Simulation and Scientific Software*
emilio@esss.com.br

1. Summary

The simulation of multiphase flows is one of the most challenging tasks for physicist and numerical analysts. For liquid-gas flows, for example, to model the interaction between gas and bubbles requires interfacial models considering the momentum and energy transfer at the gas-liquid interfaces. Among the interfacial forces, drag, virtual mass, and the so-called transversal forces, like wall lubrication and lift, are the ones most commonly taken into account. For flows with moderate contractions it suffices to consider the drag forces, and that is what is done in the majority of gas-liquid flows. However, in accelerated bubbly flows, as in venturi tubes, for example, the virtual mass and the transversal forces play important rules in predicting the pressure difference as well as the void fraction distribution in the tube cross section. This paper addresses the important issue of considering all these forces in accelerated bubbly flows. First of all, some comparisons of the model are done against experimental results. Following, it is demonstrated that the virtual mass flow has significant effect on the prediction of the pressure difference in the venturi throat, while the transversal forces have influence upon the void fraction distribution.

1.1 Introduction

The concept of virtual mass can be better understood considering Fig. 1. When a bubble flows trough a quiescent liquid, some liquid mass is carried by the bubble due to viscous interaction. This mass portion is supposed to attain the bubble velocity, resulting in a virtual increase in the bubble mass.

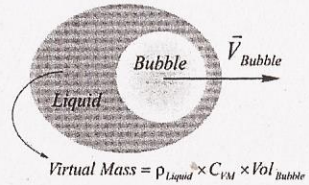

Fig. 1 – The concept of virtual mass

It is suggested in the literature that virtual mass terms should be included in order to introduce numerical stability in multiphase calculations, but which causes no influences in the flow calculations (Lahey *et al.* (1980), Geurst (1985), Watanabe & Kukita (1990)). This

is true for a large class of bubbly flows encountered in industrial problems, like constant area ducts, bubble column reactors etc., where acceleration effects are not important. On the other hand, results obtained for bubbly flows in a nozzle with high contraction ratio shows important differences in the pressure gradient calculations when virtual mass force is included in the modelling.

The aim of this work is to show the importance of considering the virtual mass and transversal forces in accelerated bubbly flows, as in venturi tube meters. The main characteristic of the flow within these devices is the strong accelerations the flow experiences along the contraction. For these cases, the correct modelling of the virtual mass force, commonly considered as a second order when compared with drag, is of fundamental importance in order to get accurate predictions for the differential pressure, which is the main variable in flow-rate metering devices.

Results for the bubbly flow in a contraction were reported in Paladino & Maliska (2004), where comparisons were made with the experimental results of Lewis & Davidson (1985). The differences between the experimental and numerical data for the differential pressure across the contraction using the two-fluid model without considering the virtual mass force can be about 10-15%, and were more evident for high void fractions. Since these are accelerated flows, it was concluded that the virtual mass effects need to be taken in consideration in order to correctly predict the pressure gradients in accelerated flows.

Virtual mass models were implemented through FORTRAN user routines available in a commercial software.

2. Mathematical Approach

Different approaches have been reported in the literature for two-phase flow modelling. However, the most popular model for the computation of multiphase flows, both in industrial and academic applications, is the so called the two-fluid model. For industrial applications, this is almost the only model used, as it is the model implemented within most commercial packages. The formulation of the two-fluid model is based on an averaging process (temporal, spatial or assemble averaging, see for example Enwald *et al.* (1996)) of the local and instantaneous mass and momentum equations for each phase and the respective interfacial conditions, given by

$$\frac{\partial}{\partial t}(\rho_i)+\nabla(\rho_i \mathbf{U}_i)=0 \tag{1}$$

$$\frac{\partial}{\partial t}(\rho_i \mathbf{U}_i)+\nabla(\rho_i \mathbf{U}_i \mathbf{U}_i-\mathbf{T}_i)=\rho \mathbf{f}_i \tag{2}$$

$$\sum_j^k(\rho_i(\mathbf{U}_i-\mathbf{U}_I)\cdot\mathbf{n}_i)=0 \tag{3}$$

$$\sum_j^k(\rho_i(\mathbf{U}_i-\mathbf{U}_I)\mathbf{U}_i\cdot\mathbf{n}_i-\mathbf{T}_i\cdot\mathbf{n}_i)=\sigma\kappa\mathbf{n}_i \tag{4}$$

The interfacial constraints, (Eqs. (3) e (4)) represents the mass and momentum balances across the interface. For the case of mass balance, there are no sources at the interface, and for the momentum equation could be imbalanced by surface tension, σ.

After the averaging process, one obtains,

$$\frac{\partial}{\partial t}(\rho_i r_i)+\nabla\cdot(\rho_i r_i \mathbf{U}_i)=\Gamma_i \tag{5}$$

$$\frac{\partial}{\partial t}(\rho_i r_i \mathbf{U}_i)+\nabla\cdot(\rho_i r_i \mathbf{U}_i \mathbf{U}_i)=\nabla\cdot\left(\mathbf{T}_i+\mathbf{T}_i^{Turb}\right)-r_i\nabla p+r_i\mathbf{f}+\mathbf{M}_{il} \tag{6}$$

where r_i is the volumetric fraction of phase i, $\mathbf{T}_i^{Turb}$ is the turbulent stress tensor of phase i and $\mathbf{M}_{il}$ is the interfacial momentum transfer term. Further details about the averaging process can be found in Drew (1983), among others texts. The averaging process of the interfacial constraints, neglecting the surface tension, leads to

$$\sum_i \Gamma_{il}=0 \tag{7}$$

$$\sum_i \mathbf{M}_{il}=0 \tag{8}$$

where Γ_{il} represents the mass fluxes through the interfaces. In this case, phase change is not considered within the model and, therefore,

$$\Gamma_{il}=\Gamma_{jl}=0 \tag{9}$$

and $\mathbf{M}_{il}$ in the interfacial momentum transfer term. The main challenge at this point is to define suitable constitutive equations for the new variable $\mathbf{M}_{il}$. Several works were published attempting to correctly define these terms. For dispersed flows the interfacial momentum transfer term is defined by analyzing the forces appearing on a body submerged in a free stream. In general, this term is given by the sum of various forces that are modelled as function of flow parameters.

Drag is the most commonly considered interfacial force. This force arrives from the viscous and pressure forces along the interface and is related to the local interfacial gradients. The influence of the drag coefficients upon the virtual mass force along a contraction can be found in Paladino and Maliska (2004). The details of the models used for representing all interfacial forces can be found in Paladino (2005).

3 – Virtual Mass Concept

The modelling of the virtual mass force is a controversial question in literature. Various constitutive equations for the modelling of the virtual mass term were published. It is of common agreement that the virtual mass force is equal to the mass of liquid carried by the bubble ($\rho_L C_{VM} V_B$) (see Fig. 1) times a suitable defined relative acceleration between phases, as

$$\mathbf{F}_{VM}=\rho_L C_{VM} V_B \mathbf{A}_{REL} \tag{10}$$

The determination of the relative acceleration is the key question involved in the modelling, and a detailed discussion on how to handle the relative acceleration and available models can be seen in Drew *et al.* (1979) and the ones used in this work can be found in Paladino (2005).

4 – Influences of Virtual Forces upon Pressure Difference and Void Fraction

In this section, results for differential pressure through the contraction as function of upstream void fraction are compared with Lewis & Davidson (1985) experimental results. This is precisely the technological target of this research, as the flow rate measured with venturi or nozzles flow-meters requires an accurate calculation of the differential pressure and void fraction upstream the device. Fig. 2 presents the pressure drop across the nozzle showed in as function of the upstream void fraction, compared with Lewis & Davidson (1985) experimental data, for liquid superficial velocities of 0.65 m/ s e 0.54 m/s.

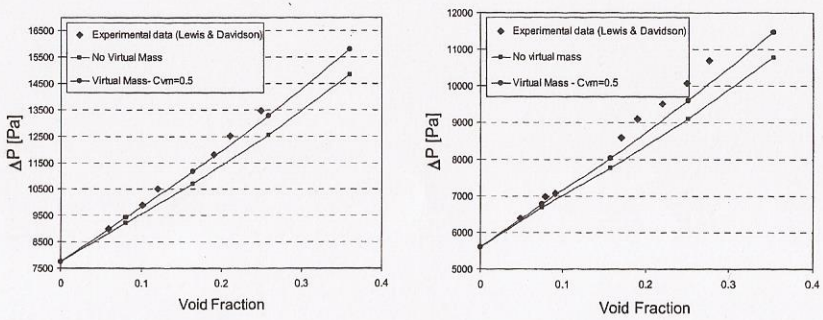

J_l = 0.65 m/s **J_l = 0.54 m/s**

Fig. 2– Differential pressure as a function of upstream void fraction with and without virtual mass force

It could be seen good agreement for low void fraction in both cases and some major differences for high void fractions for superficial velocity of 0,54 m/s. These differences are attributed to the dependence of C_{VM} on high void fractions. The introduction of the virtual mass in the calculations, significantly improves the results, indicating that this force is not negligible for accelerated flows.

4.1 - Pressure difference in venturi tubes

This section presents the solution of the flow in the venturi tube shown in Fig. 3 using 6215 control volumes. A grid with 22695 control volumes was also used, but no significant differences were encountered in the results obtained with the coarser grid for the pressure difference and void fraction distribution. The numerical results for the pressure difference across the throat will be compared with experimental results obtained in Paladino (2005). In all runs, the error defined as the Euclidian norm of the equation residual was forced to be less than 10^{-5} for all equations. Fig. 4 shows the pressure distribution along the venturi considering different combinations of interfacial forces for the following flow conditions:

Tab. 1

J_L [m/s]	J_G [m/s]	α_G	d_{Bolha} [mm]
1.03	0.15	0.1023	4.0

These conditions are the ones used by Serizawa *et al* (1975b), in one of his experiments. Results are shown for several runs considering different interfacial forces.

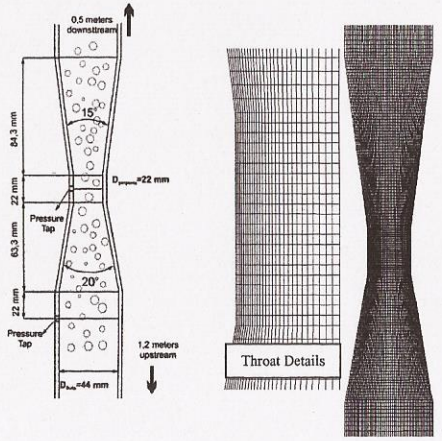

Fig. 3 - Dimensions of the venturi tube, its grid and a detail of the grid in the contraction zone

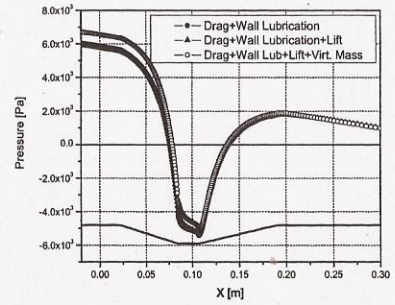

Fig. 4 – Pressure along the venturi tube considering different interfacial forces.

As already mentioned, the virtual mass force has a significant influence upon the pressure difference at the venturi throat, while the transversal forces do not. Besides the validation against the experimental results of Lewis and Davidson (1985a), the calculated

pressure difference in the venturi tube is compared with the experimental work realized in Paladino (2005).

The two-fluid model was again used considering a non-viscous dispersed phase. The interfacial forces considered are drag, with an "automatic" calculation of the drag coefficient based on the bubble Reynolds number, virtual mass, wall lubrication and lift. Superficial velocities for each phase were specified. The void fraction at the entrance was estimated considering fully developed flow of water and air with the bubble attaining their terminal velocity. To guarantee these conditions the computational domain was extended upstream around 40 diameters. Details and all equations representing the models used herein can be found in Paladino (2005).

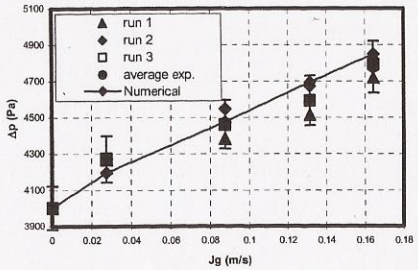

Fig. 5 – Numerical versus experimental results for the venturi tube

Fig. 5 shows good agreement between the numerical and experimental results for the pressure difference versus superficial air velocity for J_L = 0,62 m/s. Coefficients employed are given in Table 2. Results for others values of liquid superficial velocities can be found in Paladino (2005). The error bars consider an approximate error in the measurements of about 3%, calculated considering only the uncertainty of the pressure transducer. This uncertainty is damped by the average of 3000 measurement taken in each test. Surprisingly, larger errors are predicted for larger superficial gas velocities, opposed to what was observed by Lewis and Davidson (1985a). This finding was not yet clarified.

Tab. 2 – Coefficients employed in the interfacial forces

C_D	C_L	C_{VM}	$-C_{W1}$, C_{W2}
Automatic	0.1	0.5	0.02, 0.04

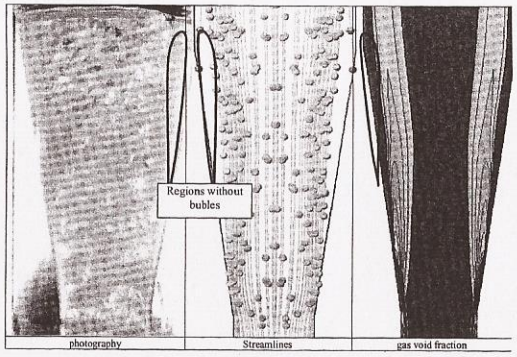

Fig. 6 – Qualitative experimental results compared with the numerical calculations for the void fraction distribution

It can be seen in Fig. 6 that the experimental visualization of the void fraction distribution agrees well with the numerical results. Regions without bubbles marked in Fig. 6 are well predicted by the model. In order to analyze the influences of the different forces in the void fraction distribution, five cases were simulated, shown in Tab. 3, considering the transversal, lift and wall lubrication, and turbulent dispersion forces.

Tab. 3 – Coefficients for the transversal and turbulent dispersion forces.

Case	C_L	C_{TD}	$-C_{W1}$, C_{W2}
1	0.06	0.02	0.025, 0.05
2	0.1	0.02	0.025, 0.05
3	0.1	0.1	0.025, 0.05
4	0.25	0.1	0.025, 0.05
5	0.0	0.1	0.025, 0.05

In Case 1 the coefficients given by Troshko & Hassan (2001b) for constant cross section ducts was used, and it was concluded that better results are found when C_L = 0.1. Fig. 7 shows the transversal profiles for the void fraction for three positions along the venturi tube, compared with the results of Thang and Davis (1979).

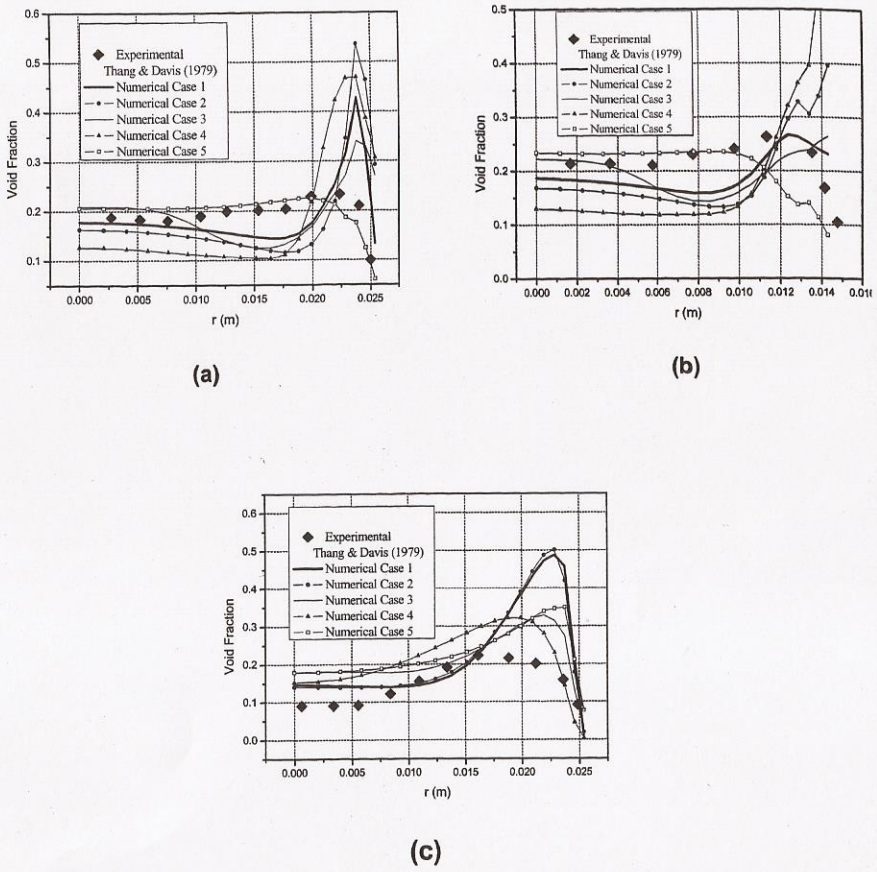

Fig. 7 – Transversal profiles for void fraction: (a) Entrance; (b) throat and (c) outlet

For the profiles at the entrance and at the throat, Case 5, which does not consider the lift force, better represent the experimental profiles. However, in the throat, Case 1 shows better agreement close to the wall. For the outlet profiles, all cases present some discrepancy with the experimental results. In this section, the best case, at least qualitatively, was obtained with Case 4, where a relatively large value for the lift coefficient was considered. This is because, as we could see by the visualization, bubbles tend to leave the wall due to the changing in the sign of the lift force in the diverging part of the venturi. However, Case 4 could not represent well the profiles at the inlet and throat. The outcome of the analysis suggests that it may be necessary to have the lift coefficient tied to the flow

properties. Not considering the wall lubrication force also causes the detachment of the boundary layer, changing drastically the local void fraction. These findings demonstrates that the wall lubrication forces although does not influences the pressure difference, significantly alters the void fraction distribution. Not considering lubrication causes peaks in the void fraction distribution. Not considering the lift forces the bubbles are not forced to the center, as experimentally observed.

5. Concluding Remarks

Virtual mass force significantly affects the pressure gradients because part of the liquid with greater density is accelerated up to the bubbles velocity and the pressure gradient required to accelerate the whole mixture is increased. Or, from other point of view, the dispersed (lighter) phase "sees" its mass increased by the virtual mass and the pressure gradient required to accelerate it is larger and so will be the pressure gradient required to accelerate the whole mixture. Results show that the inclusion of this force in the calculations goes beyond stability considerations.

Results for velocity profiles along the contraction show that inclusion of virtual mass practically does not affect velocity fields. For the two-fluid model this is expected, as average phase velocities are subjected to the constraint of mass conservation although in a physical reasoning, virtual mass implies that part of liquid is accelerated to the gas phase velocity, and this would increase the average liquid velocity.

Regardless of what is the better formulation for the virtual mass force, the main goal of this work was to demonstrate that in accelerated bubbly flows the virtual mass can play a very important role, depending on the magnitude of accelerations present on flow. Transversal forces need also to be considered, since they act in distributing the bubbles near walls, changing the local void fraction profiles.

Nomenclature

r_i	Volumetric fraction of phase *i*
$\mathbf{U}_i$	Velocity of phase *i*
$\mathbf{U}_0$	Interstitial liquid velocity (Three field model)
$\mathbf{U}_I$	Velocity of the interface
U_T	Terminal bubble velocity
J_l, J_g	Liquid and gas superficial velocities ($=r_l U_l$, $r_g U_g$)
C_{VM}	Virtual mass coefficient
C_D	Drag coefficient
$\mathbf{F}_I$	Interfacial force (Lagrangean framework)
$\mathbf{M}_I$	Interfacial momentum transfer term (Eulerian framework)
V_b	Bubble volume
d	Bubble diameter
g	Gravity acceleration (modulus)
λ	Parameter for objectivity in relative acceleration
σ	Surface tension
κ	Interfacial curvature in the local interfacial constraints
Γ_{il}	Averaged mass flux trough the interface

References

1. Drew, D., Cheng, L., and Lahey, J., "The analysis of virtual mass effects in two-phase flow," *International Journal of Multiphase Flow*, Vol. 5, No. 4, 1979, pp. 233-242.
2. Drew, D., "Mathematical modelling of two-phase flows," *Annual Review of Fluid Mechanics*, Vol. 15, 1983, pp. 261-291.
3. Drew, D. A. and Lahey, J., "The virtual mass and lift force on a sphere in rotating and straining inviscid flow," *International Journal of Multiphase Flow*, Vol. 13, No. 1, 1987, pp. 113-121.
4. Enwald, H., Peirano, E., and Almstedt, A.-E., "Eulerian two-phase flow theory applied to fluidization," *International Journal of Multiphase Flow*, Vol. 22, No. 1, 1996, pp. 21-66.
5. Geurst, J. A., "Virtual mass in two-phase bubbly flow," *Physica A: Statistical and Theoretical Physics*, Vol. 129, No. 2, 1985, pp. 233-261.
6. Karema, H. and Lo, S., "Efficiency of interphase coupling algorithms in fluidized bed conditions," *Computers & Fluids*, Vol. 28, No. 3, 1999, pp. 323-360.
7. Krishna, R., Urseanu, M. I., van Baten, J. M., and Ellenberger, J., "Rise velocity of a swarm of large gas bubbles in liquids," *Chemical Engineering Science*, Vol. 54, No. 2, 1999, pp. 171-183.
8. Lahey, J., Cheng, L. Y., Drew, D. A., and Flaherty, J. E., "The effect of virtual mass on the numerical stability of accelerating two-phase flows," *International Journal of Multiphase Flow*, Vol. 6, No. 4, 1980, pp. 281-294.
9. Lewis, D. A. and Davidson, J. F., "Pressure drop for bubbly gas-liquid flow through orifice plates and nozzles," *Chem.Eng.Res.Des.*, Vol. 63, 1985, pp. 149-156.
10. Paladino, E. E. and Maliska C.R.. The Effect of the Slip Velocity on the Differential Pressure in Multiphase Venturi Flow Meters. IPC'02 - International Pipeline Conference, Calgary, Alberta, Canada, September 29 – October 3, 2002.
11. Paladino. E., E., (2005), "Estudo do Escoamento Multifásico em Medidores de Vazão do Tipo Pressão Diferencial" Ph.D. Thesis, Mechanical Engineering Department, UFSC, Brasil.
12. Paladino, E. E., Maliska, C.R., (2004), Virtual Mass is Accelerated Bubbly Flows, Proceedings of the 4th European Thermal Sciences, 29th-31st March, National Exhibition Centre, Birmingham, UK.
13. Van Doormaal, J. P. and Raithby, G. D., "Enhancements of the SIMPLE method for predicting incompressible fluid flows," *Numerical Heat Transfer*, Vol. 7, 1984, pp. 147-163.
14. Wallis, G. B., *One-dimensional two-phase flow*, McGraw-Hill, New York 1969.
15. Watanabe, T. and Kukita, Y., "The effect of the virtual mass term on the stability of the two-fluid model against perturbations," *Nuclear Engineering and Design*, Vol. 135, No. 3, 1992, pp. 327-340.

Acknowledgements

This work was partially supported by the Brazilian National Petroleum Agency-ANP and FINEP, through the PRH09-Human Resources Program in Petroleum and Gas.